

# The future of brain–machine interfaces is optical

Nathan Tessema Ersaro, Cem Yalcin & Rikky Muller



Optical interfaces could be used to address challenges related to scaling, precision and invasiveness in the development of brain–machine interfaces.

Advances in brain–machine interfaces (BMIs) have been driven by a proliferation of neural sensing and stimulating modalities, as well as an increase in the number of neurons that can be simultaneously recorded. These advances have led to new insights into neural systems and the development of novel clinical tools. In basic research, BMIs allow neuroscientists to explore the interplay between brain–behaviour causality and self-observation, and to study neural plasticity, coding and pathophysiology<sup>1</sup>. In applied research, BMIs can help patients with limited ability to communicate and patients with restricted motor function<sup>2</sup>.

Ideally, a BMI should be minimally invasive, extremely safe and offer sufficient longevity. It should have a feedback system to close the communication loop. It should also have high spatiotemporal resolution and throughput for communication depth to enable both complex brain encoding (via arbitrary and precise neurostimulation patterns) and brain decoding (via sufficiently large readout data with precise features)<sup>3</sup>. However, the human brain has roughly 80 billion neurons, with a density of around  $10^5$  neurons per  $\text{mm}^3$  (ref. <sup>4</sup>). Thus, the trade-off between spatial scale and resolution has emerged as a key challenge in achieving meaningful communication with the tissue regions responsible for sensory, motor and cognitive functions in the central nervous system.

Non-invasive BMIs avoid surgery and can ensure longevity by employing external tools for recording (such as electroencephalography (EEG)) and stimulation (such as transcranial magnetic stimulation)<sup>5</sup>. However, this approach has fundamental limits in terms of communication complexity since the measurements constitute summed electrical signals recorded from a distance (true of EEG and also electrocorticography, where electrodes are placed on the surface of the cortex) and since stimulation targets relatively large volumes of tissue.

Microelectrodes surgically inserted into brain tissue can be used to record signals with the resolution of a single neuron and to perform intracortical microstimulation. However, even such high-precision microelectrodes have only been able to perform concurrent recording on up to hundreds of distinct neurons<sup>6</sup>. In addition, the longevity, reliability and safety of such electrode arrays is limited by physical damage during insertion, the immune response to the implant and the reorganization of neural circuits over time. While it has been suggested that it may be possible to simultaneously electrically record from every neuron in a mammalian cortex<sup>7</sup>, charge density limits rule out safe stimulation at the proposed electrode size<sup>8</sup>.

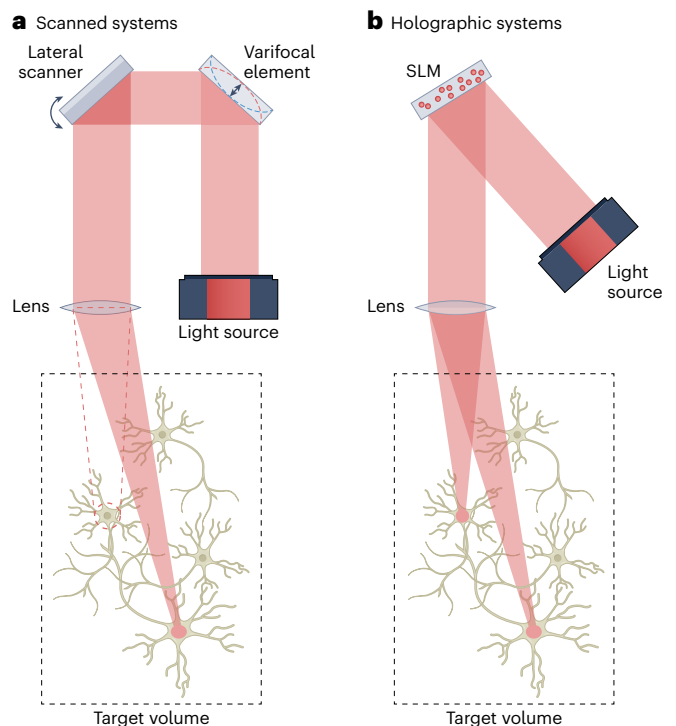


**Fig. 1 | Volumetric patterning in optical neural interfaces.** **a**, Optical diagram for scan-based light delivery systems. A varifocal element for axial scanning is complemented with a lateral scanner to precisely position a focused spot of light across the target volume. **b**, Optical diagram for holographic light delivery systems. An SLM imprints a phase mask onto an incident laser beam, which forms the desired 3D point cloud intensity distribution through downstream interference. Credit: © 2022 IEEE. Reprinted, with permission, from ref. <sup>31</sup>.

Optics could provide an answer here. The advent of gene editing has enabled the development of fluorescent voltage indicators located within neuron membranes that track individual firing events<sup>9</sup> and actuating proteins known as opsins that respond to light by triggering or inhibiting neuron firing<sup>10</sup>. Thus, through the use of cranial windows, both recording and stimulation can be performed across different optical wavelengths to avoid read–write crosstalk and without physically penetrating brain tissue. With such methods, optical neural interfaces can precisely control and interrogate mammalian neural circuits, creating BMIs that can achieve stimulation patterns capable of driving realistic sensory precepts<sup>11</sup>. The precision offered by optical neural interfaces is further aided by auxiliary techniques, including multiphoton excitation and temporal focusing, which can confine illuminated target regions<sup>12</sup>. In addition, existing bottlenecks

with optical methods – including photoresponse kinetics, off-target effects and tissue heating – are being targeted by ongoing innovations in biological probe engineering<sup>13,14</sup>.

## The dual challenge of precision and throughput

To fully exploit the level of targeting precision offered by optical BMs, volumetric patterning at neuron-soma-level resolution (around 10  $\mu\text{m}$ ) is required in both fluorescent excitation of indicator probes<sup>15</sup> (for imaging) and optogenetic activation of opsins (for photostimulation)<sup>10</sup>. Previous studies have achieved such dynamic optical patterning through three-dimensional (3D) point scanning methods (Fig. 1a)<sup>16</sup>. Yet despite speeds that exceed the kilohertz timescales of neuronal activity, the serial nature of point scanning precludes concurrent addressing, which severely limits targeting throughput.

Parallel addressing via computer-generated holography has thus emerged as a popular approach to photostimulation and imaging in neuroscience (Fig. 1b)<sup>11</sup>. In such systems, dynamic holographic projection is achieved using a spatial light modulator (SLM). This is typically a configurable diffractive surface, such as an optical phased-array surface, capable of imparting pixel-level phase and amplitude modulation to a coherent input beam in order to generate desired 3D illumination patterns via downstream interference. Holographic patterning efforts in neuroscience have demonstrated the ability to target up to 750 neurons with a single frame of a 0.5-megapixel SLM<sup>10</sup>. Several studies have also employed computer-generated holography patterning jointly with raster scanning for expanded system capabilities, including an extended field of view<sup>17</sup> and spiral beam tracing across neuron soma for stronger photostimulation<sup>11</sup>.

Ensuring precision in optical neural interfaces also entails eliminating the impact of motion artefacts and aberrations from scattering in neural tissue via dynamic wavefront shaping<sup>18</sup>. Such shaping is typically achieved using kilohertz-rate adaptive optics tools such as continuous deformable mirror arrays<sup>19</sup>. Ideally, all point-cloud patterning and aberration-correction functionality across imaging and photostimulation would be consolidated to one SLM for optimal compactness. However, this requires SLM refresh rates that match those of adaptive optics tools, which highlights the importance of modulation speed in optical neural interfaces.

Moreover, a fundamental consideration with SLMs is that the available space–bandwidth product, given by SLM pixel count, is only conserved when patterning across a single depth plane, such that SLM pixel count scales linearly with the number of possible targets per SLM frame. When patterning is extended to a 3D volume consisting of multiple depth planes, a space–bandwidth product mismatch emerges, with larger SLM formats that target more spots per frame suffering from diminishing performance in terms of optical efficiency and image fidelity. Therefore, operating the SLM at a higher frame rate with fewer targets per SLM frame would improve efficiency and fidelity as a result of reduced unwanted interference between beamlets targeting different neurons, making SLM speed doubly important to the deployment of optical BMs.

In practice, the minimum allowable SLM switching period is given by the sum of the SLM settling time (during which illumination is turned off) and the response time for photostimulation with opsins or for indicators such as genetically encoded voltage indicators (during which illumination is turned on)<sup>20</sup>. Eclipsing the impact of SLM switching times for millisecond-scale biological probes requires SLM speeds in excess of 10 kHz. Yet, although recent opsins and genetically encoded voltage indicators have entered the regime of kilohertz-rate kinetics<sup>13,14</sup>,

state-of-the-art commercially available SLMs continue to suffer from bottleneck speeds of less than 500 Hz due to the optofluidic settling of liquid-crystal-based phase-modulating pixels<sup>21</sup>.

The critical need for high-speed SLMs in optical BMs therefore remains unmet. Importantly, pixel count requirements for such high-speed SLMs need not match the megapixel regime of current liquid-crystal-on-silicon SLMs<sup>21</sup>, as even pixel counts on the order of  $10^4$  (that is, around  $100 \times 100$ ) would be capable of matching state-of-the-art targeting throughput performance with 10 kHz speed. Any available excess refresh rate may also be used to further improve image fidelity and signal-to-noise ratio via time-averaged speckle reduction<sup>22</sup>.

## Opportunities for hardware and electronics

Several technologies are being explored for kilohertz-to-megahertz-rate array-scale phase modulation. These include ferroelectric liquid crystals<sup>23</sup>, silicon photonic phased arrays employing thermo-optic or microelectromechanical system (MEMS)-based phase shifters<sup>24</sup>, and tunable metasurfaces and resonant optical antennas<sup>25</sup>. Yet challenges hampering array scaling and functional deployment persist as these technologies achieve high SLM speeds at the expense of various trade-offs, including binary-only phase modulation in ferroelectric liquid crystals<sup>23</sup>, high power consumption in thermo-optic phase shifters<sup>24</sup>, large size and insertion loss in MEMS-based photonic MEMS shifters<sup>24</sup>, and limited or co-dependent phase and amplitude modulation in tunable nanoantennas<sup>25</sup>.

Nevertheless, advanced commercialization efforts for high-speed SLMs exist, particularly around piston-motion electrostatically actuated micromirror arrays, which underpin existing products such as continuous deformable mirror arrays<sup>26</sup> and grating light valves<sup>27</sup>. Similarly, Texas Instruments recently leveraged its surface micromachined complementary metal–oxide–semiconductor (CMOS) platform for digital micromirror devices to develop a phase light modulator SLM<sup>28</sup>. These SLMs typically exhibit large pixel pitches on the order of tens of micrometres, which limits native SLM field of view and requires demagnification optics. However, phase-shifting micromirror arrays are promising as high-speed SLMs because they can surpass 10 kHz refresh rates, allow for random-access patterning via quasi-static operation, and are agnostic to polarization, which is not the case for liquid crystals and metasurfaces<sup>28,29</sup>.

Regardless of the underlying technology, the use of high-speed SLMs to increase optical targeting throughput requires an electronic addressing scheme with sufficiently dense integration to simultaneously drive all available degrees of freedom (that is, pixels) and with sufficient bandwidth to achieve settling limited only by the phase-modulation mechanism. Off-the-shelf driver solutions often fail to fully mobilize SLM capabilities, bottlenecking refresh rate and modulation depth<sup>28</sup>, or employ inefficient integration schemes, resulting in heavy and cumbersome form factors<sup>30</sup>. Accordingly, a tight co-design process between an SLM array and integrated circuit driver is required in order to achieve a level of tailorability that can alleviate driver burden for nimble, low-power and compact operation. For example, customized digital-to-analogue converter architectures could be employed to avoid wasted drive precision for nonlinear phase-modulation behaviour, which is common in piston-motion micromirror arrays<sup>29,31</sup>.

Custom drivers could also be used to automate typically onerous global or local calibration approaches, which are often required post-fabrication due to mismatches across SLM pixels and arrays<sup>25,31</sup>. Lastly, operating smaller SLMs at higher speeds could allow for on-chip

real-time computation of SLM phase masks. Indeed, since phase-mask computation relies on fast Fourier transform operations, which scale with  $N \times \log N$  (where  $N$  is the total SLM pixel count)<sup>22</sup>, fast and small SLMs offer improvements of several orders of magnitude in terms of compute time compared with large but slow SLMs for a given targeting throughput.

Safety, longevity and portability pose considerable challenges for the development of BMIs. These issues could be improved through the use of optically transparent, hermetically sealed cranial windows under all-optical schemes<sup>32</sup>. Yet, whereas optogenetics has entered the clinical realm, clinical implementations of all-optical BMIs remain out of reach with current capabilities. Nevertheless, the precise level of control that patterned illumination offers for the manipulation of neural activity has opened up an entirely new class of experiments to interrogate neural circuits and elucidate gaps in our understanding of neural coding<sup>33</sup>.

**Nathan Tessema Ersaro**<sup>1</sup>, **Cem Yalcin**<sup>2</sup> & **Rikky Muller**<sup>1,2</sup> ✉

<sup>1</sup>Graduate Program in Bioengineering, University of California, Berkeley and University of California, San Francisco, Berkeley, CA, USA. <sup>2</sup>Department of Electrical Engineering and Computer Sciences, University of California, Berkeley, Berkeley, CA, USA.

✉ e-mail: [rikky@berkeley.edu](mailto:rikky@berkeley.edu)

Published online: 17 February 2023

## References

1. Moxon, K. A. & Foffani, G. *Neuron* **86**, 55–67 (2015).
2. Lee, M. B. et al. *J. Clin. Neurosci.* **68**, 13–19 (2019).
3. Murphy, M. D., Guggenmos, D. J., Bundy, D. T. & Nudo, R. J. *Front. Cell. Neurosci.* **9**, 497 (2016).
4. Marblestone, A. H. et al. *Front. Comput. Neurosci.* **7**, 137 (2013).
5. Zrenner, C., Belardinelli, P., Müller-Dahhaus, F. & Ziemann, U. *Front. Cell. Neurosci.* **10**, 92 (2016).
6. Juavinett, A. L., Bekheet, G. & Churchland, A. K. *eLife* **8**, e47188 (2019).
7. Kleinfeld, D. et al. *Neuron* **103**, 1005–1015 (2019).
8. Merrill, D. R., Bikson, M. & Jefferys, J. G. R. *J. Neurosci. Methods* **141**, 171–198 (2005).
9. Gong, Y. et al. *Science* **350**, 1361–1366 (2015).
10. Pégard, N. C. et al. *Nat. Commun.* **8**, 1228 (2017).
11. Marshel, J. H. et al. *Science* **365**, eaaw5202 (2019).
12. Papagiakoumou, E., Ronzitti, E. & Emiliani, V. *Nat. Methods* **17**, 571–581 (2020).
13. Ronzitti, E. et al. *J. Neurosci.* **37**, 10679–10689 (2017).
14. Villette, V. et al. *Cell* **179**, 1590–1608 (2019).
15. Chamberland, S. et al. *eLife* **6**, e25690 (2017).
16. Sakaki, K. D. R., Podgorski, K., Dellazzio Toth, T. A., Coleman, P. & Haas, K. *Front. Neural Circ.* **14**, 33 (2020).
17. Go, M. A., Mueller, M., Castañares, M. L., Egger, V. & Daria, V. R. *PLoS ONE* **14**, e0210564 (2019).
18. Gigan, S. et al. *J. Phys. Photon.* **4**, 42501 (2022).
19. Li, Z. et al. *Sci. Adv.* **6**, eaaz3870 (2020).
20. Mardinly, A. R. et al. *Nat. Neurosci.* **21**, 881–893 (2018).
21. Shane, J. C., McKnight, D. J., Hill, A., Taberski, K. & Serati, S. In *Proc. Optical Trapping and Optical Micromanipulation XVI* (eds Dholakia, K. & Spalding, G. C.) Vol. 11083, 3 (SPIE, 2019).
22. Eybposh, M. H., Curtis, V. R., Rodríguez-Romaguera, J. & Pégard, N. C. *Neurophotonics* **9**, 41409 (2022).
23. Schmieler, F. et al. *Appl. Sci.* **8**, 1180 (2018).
24. Sun, H., Qiao, Q., Guan, Q. & Zhou, G. *Micromachines* **13**, 1509 (2022).
25. Panuski, C. L. et al. *Nat. Photon.* **16**, 834–842 (2022).
26. Norton, A. et al. In *MEMS Adaptive Optics III* (eds Olivier, S. S. et al.) Vol. 7209, 134–140 (SPIE, 2009).
27. Landry, J., Hamann, S. & Solgaard, O. *J. Biomed. Opt.* **25**, 106504 (2020).
28. Bartlett, T. A. et al. In *Emerging Digital Micromirror Device Based Systems and Applications XIII* (eds Ehmke, J. & Lee, B. L.) Vol. 11698, 103–116 (SPIE, 2021).
29. Ersumo, N. T. et al. *Light Sci. Appl.* **9**, 183 (2020).
30. Bendek, E. A. et al. *J. Astron. Telesc. Instrum. Syst.* **6**, 45001 (2020).
31. Yalcin, C. et al. *IEEE J. Solid-State Circuits* **57**, 3442–3452 (2022).
32. Kim, T. H. et al. *Cell Rep.* **17**, 3385–3394 (2016).
33. Adesnik, H. & Abdeladim, L. *Nat. Neurosci.* **24**, 1356–1366 (2021).

## Competing interests

The authors declare no competing interests.